

an phagocytic cells and generates therein very large amounts of cyclic AMP. This, in turn, suppresses a variety of neutrophil and macrophage functions including superoxide production, chemotaxis, and bacterial killing. This phenomenon probably explains previous observations of alveolar macrophage dysfunction in *B. bronchiseptica*-infected rabbits and may explain the greatly increased susceptibility to secondary bacterial pneumonias seen in *B. pertussis*-infected humans. Our observations may also help elucidate the pathogenesis of atrophic infectious rhinitis in pigs, a chronic *Bordetella* infection in which there is agenesis and dissolution of the turbinate bones within the snout. Indeed, programmed elevations of cyclic AMP have been implicated in the atrophy and loss of certain cell types during normal morphogenesis (19).

The *Bordetella* adenylate cyclase probably represents an important adaptive strategy for the bacterium, in that suppression of host phagocytic response will permit the survival and replication of an otherwise vulnerable organism. *Bordetella* accomplishes this through the purposeful misuse of a control system that normally operates as a negative modulator of various cellular functions. We anticipate that this unusual bacterial adenylate cyclase will add to our understanding of the pathogenesis of *Bordetella* infections. This enzyme may be used to manipulate intracellular cyclic nucleotide metabolism in a variety of experimental and, perhaps eventually, clinical situations.

DENNIS L. CONFER  
JOHN W. EATON

Departments of Medicine and  
Laboratory Medicine/Pathology,  
University of Minnesota Medical  
School, Minneapolis 55455

#### References and Notes

1. J. A. Walsh and K. S. Warren, *N. Engl. J. Med.* **301**, 967 (1979).
2. L. C. Olson, *Medicine (Baltimore)* **54**, 427 (1975).
3. J. R. Hoidal, G. D. Beall, F. L. Rasp, B. Holmes, J. G. White, J. E. Repine, *J. Lab. Clin. Med.* **92**, 878 (1978).
4. E. L. Hewlett, M. A. Urban, C. R. Manclark, J. Wolff, *Proc. Natl. Acad. Sci. U.S.A.* **73**, 1926 (1976); E. L. Hewlett and J. Wolff, *J. Bacteriol.* **127**, 890 (1976); M. Endoh, T. Takezawa, Y. Nakase, *Microbiol. Immunol.* **24**, 95 (1980).
5. H. R. Bourne, R. I. Lehrer, M. J. Cline, K. L. Melmon, *J. Clin. Invest.* **50**, 920 (1971); E. Pick, *Nature (London) New Biol.* **238**, 176 (1972); J. D. Cox and M. L. Karnovsky, *J. Cell Biol.* **59**, 480 (1973); C. W. Parker, T. J. Sullivan, H. J. Wedner, *Adv. Cyclic Nucleotide Res.* **4**, 1 (1974); H. R. Bourne, L. M. Lichtenstein, K. L. Melmon, C. S. Henney, Y. Weinstein, G. M. Shearer, *Science* **184**, 19 (1974); M. Roch-Arveiller, P. Boquet, D. Bradshaw, J. P. Giroud, *Infect. Immunol.* **25**, 187 (1979).
6. Peripheral blood neutrophils were obtained by dextran sedimentation of heparinized venous blood followed by Ficoll-hypaque density separation [J. E. Repine, J. W. Eaton, M. W. An-

- ders, J. R. Hoidal, R. B. Fox, *J. Clin. Invest.* **64**, 1642 (1979)].
7. *Bordetella pertussis* (ATCC strain e9340, obtained from the American Type Culture Collection) was first cultured on Bordet-Gengou agar and inocula from these cultures were then grown in chemically defined medium [D. W. Stainer and M. J. Scholte, *J. Gen. Microbiol.* **63**, 211 (1971)]. After 24 to 48 hours of growth, the organisms and cell-free supernatant were separated by centrifugation at 10,000g for 30 minutes.
  8. L. Simchowicz, J. P. Atkinson, I. Spilberg, *J. Clin. Invest.* **66**, 736 (1980). The apparent inhibition of superoxide production might be caused by the presence of superoxide dismutase (SOD). However, direct measurements of SOD [J. M. McCord, J. D. Crapo, I. Fridovich, in *Superoxide and Superoxide Dismutases*, A. M. Michelson, J. M. McCord, I. Fridovich, Eds. (Academic Press, New York, 1977), pp. 11-17] failed to reveal detectable activity in any of the *Bordetella* preparations used.
  9. *Bordetella pertussis* organisms (7) enriched to  $\sim 10^{11}$  per milliliter by centrifugation, were admixed with urea to 4M while being stirred constantly, and then were stored at  $-70^{\circ}\text{C}$ . Immediately before use, these extracts were dialyzed at  $4^{\circ}\text{C}$  against 2000 volumes of phosphate-buffered saline, pH 7.4, for 18 hours to remove the urea. Insoluble material was removed by centrifugation for 30 minutes at 20,000g. The possibility that residual urea or contaminants therein might account for some of the inhibitory effects was ruled out by incubating control cells with (i) Stainer-Scholte growth medium treated in parallel with the bacterial culture, (ii) equivalent volumes of the external dialysis fluid, and (iii) concentrations of urea up to 50 mM. None of these inhibited the neutrophil response to opsonized zymosan or phorbol myristate acetate.
  10. Alveolar macrophages were obtained from bronchial lavage performed on normal volunteers and on patients undergoing bronchoscopy for diagnostic purposes. The cells obtained from such lavage fluids were > 93 percent macrophages as assessed by microscopic examination of stained smears and, in some cases, by non-specific esterase stain [S. B. Tucker, R. V.

- Pierre, R. E. Jordan, *J. Immunol. Meth.* **14**, 267 (1977)].
11. S. R. Meshnick and J. W. Eaton, *Biochem. Biophys. Res. Commun.* **102**, 970 (1981).
  12. P. J. Quie, J. G. White, B. Holmes, R. A. Good, *J. Clin. Invest.* **46**, 668 (1967).
  13. S. Utsumi, S. Sonoda, T. Imagawa, M. Kanoh, *Biken J.* **21**, 121 (1978); T. Imagawa, S. Sonoda, M. Kanoh, S. Utsumi, *ibid.* **22**, 1 (1979).
  14. S. Levine and R. Sowers, *Am. J. Pathol.* **67**, 349 (1972); W. R. Benjamin, T. W. Klein, S. H. Pross, H. Friedman, *Proc. Soc. Exp. Biol. Med.* **166**, 249 (1981).
  15. The *B. pertussis* adenylate cyclase activity was assayed as described [E. L. Hewlett, L. H. Underhill, G. H. Cook, C. R. Manclark, J. Wolff, *J. Biol. Chem.* **254**, 5602 (1979)]. The reaction mixture contained 10 to 50  $\mu\text{g}$  of bacterial protein, 5 mM adenosine triphosphate, 10 mM  $\text{MgCl}_2$ , and, per milliliter, 25  $\mu\text{g}$  of membrane-free red blood cell lysate (as a source of calcium-dependent regulatory protein) in Hanks balanced salt solution. The mixture was incubated at  $37^{\circ}\text{C}$  for 10 minutes and stopped by the addition of an equal volume of 10 percent trichloroacetic acid. Cyclic AMP was then determined (16).
  16. B. L. Brown, R. P. Ekins, J. D. M. Albano, *Adv. Cyclic Nucleotide Res.* **2**, 25 (1972).
  17. Results obtained by others (15), which we have substantiated, indicate that *B. pertussis* adenylate cyclase activity is totally destroyed by incubation with as little as 50  $\mu\text{g}$  of trypsin per milliliter at pH 7.4 for 5 minutes at  $37^{\circ}\text{C}$ . Survival of this enzyme after trypsin treatment, therefore, indicates that the cyclase is intracellular.
  18. E. L. Hewlett, G. A. Myers, K. T. Saner, S. A. Long, R. L. Guerrant, *Clin. Res.* **30**, 368A (1982).
  19. R. M. Pratt and G. R. Martin, *Proc. Natl. Acad. Sci. U.S.A.* **72**, 874 (1975).
  20. We thank J. R. Sheppard and J. Haldane for helpful discussions, J. McSwigan for cyclic AMP assays, and M. Leida and B. Nelson for technical help. D.L.C. is supported by a NIH training grant (5T32-H L07062), and J.W.E. is the recipient of an NIH Research Career Development Award.

25 May 1982

## Initiation of Endochondral Calcification Is Related to Changes in the Redox State of Hypertrophic Chondrocytes

**Abstract.** *The level of pyridine nucleotides (NADH and NAD<sup>+</sup>) in the mineralizing growth plate of the chick was ascertained by high-resolution scanning microfluorimetry and biochemical analysis. Scanning electron microscopy and light microscopy were used to relate the concentrations of NADH and NAD<sup>+</sup> to stages of chondrocyte maturation. A dramatic increase was found in the relative concentration of reduced pyridine nucleotides in the hypertrophic zone. On either side of this zone, in proliferating and calcifying cartilage, there was a decrease in NADH fluorescence, and the NADH/NAD<sup>+</sup> ratio was depressed. The finding that NADH accumulated in the tissue zone associated with the earliest deposition of bone mineral supports the hypothesis that a change in the redox state initiates tissue mineralization.*

Studies of the epiphyseal growth plate have shown that, during the mineralization process, chondrocytes undergo sequential metabolic and developmental changes. In the premineralizing regions of the plate, cells concentrate inorganic ions in their mitochondria (1). At the calcification front, cellular  $\text{Ca}^{2+}$  and phosphate ( $\text{P}_i$ ) efflux is related to the low tissue  $\text{O}_2$  tension (2). Ion efflux may also result from the accumulation of phosphoenolpyruvate. This glycolytic intermediate is found in high levels in hypoxic cells and can induce  $\text{Ca}^{2+}$  release from isolated chondrocyte mitochondria (3). Thus, several lines of investigation sug-

gest that cell ion discharge and mineral deposition is associated with hypoxia-related events.

Experimental support for the concept that redox conditions directly modulate endochondral mineralization is largely inferential. While there have been measurements of normal respiratory activity as well as measurements of glycolytic and pentose shunt pathways in chondrocytes, there are neither calculated values nor direct determinations of redox-sensitive components (4). We have combined biochemical and morphological techniques to measure the major redox couple of cells in the growth plate. The

experiment reveals that there are zone-specific differences in the relative distribution of pyridine nucleotides, with a marked increase in the reduced form of nicotinamide adenine dinucleotide (NADH) in the zone of hypertrophic cartilage. Thus, NADH accumulates in a tissue zone previously shown to be hypoxic and in which mineralization is first seen.

The metabolic state of the tissue was ascertained by using scanning microfluorimetry to record fluorescence signals from chondrocyte mitochondria. The principle of this technique is that when NADH is excited with light at 366 nm it emits light with a peak intensity of about 460 nm (5). At these wavelengths, NAD<sup>+</sup> and nicotinamide adenine dinucleotide phosphate (NADP) have only a small fluorescence yield. The morphology of the tissue can be related to NADH fluorescence by scanning electron microscopy (SEM). The concentration of both NADH and NAD<sup>+</sup> in 90- $\mu$ m tissue slices was also measured biochemically

by a sensitive enzyme cycling procedure and correlated with the tissue slice morphology.

White Rock chicks, 6 to 8 weeks old, were killed by cervical dislocation. The legs were immediately frozen in liquid nitrogen, skin and flesh were removed, and the tibia and fibula were exposed by blunt dissection. The epiphyseal zones were revealed by freeze-fracturing the bone. Pieces of the frozen growth plate, measuring about 5 by 15 mm, were milled to yield a flat surface, and three small holes were drilled into selected regions of the plate to serve as fiducial points. These holes facilitated correlation of the distribution of the fluorescent spectra with the tissue morphology.

For the microfluorimetry measurements, a computer directed an 80- $\mu$ m lightguide, connected to a time-sharing fluorimeter, across the growth plate surface in a raster of points 100  $\mu$ m apart. At each point in the raster, the fluorescence intensity of NADH (Fig. 1A) was measured with a computer-linked scan-

ner and was displayed on a television monitor (6). Nonspecific effects were ruled out by recording phosphorescence measurements 4 msec after excitation at 366 nm. Although some phosphorescence was elicited, it was insufficient to mask the fluorescence signals of the plate.

After the fluorescence scan, the samples were dehydrated with acetone, critical point-dried, and sputter-coated with gold. With the drill holes as guides, SEM montages were made to correlate the fluorescence spectra with growth plate morphology.

A low-power view of the growth plate (Fig. 1B) shows the positions of the three drill holes, which can be related to the fluorescence scan of the tissue (Fig. 1A). Drill hole 1 is in the premineralized resting and proliferating zones (Fig. 1, C and D). Drill hole 2 is located at the junction of the late hypertrophic and calcifying cartilage (Fig. 1E). It is in the late hypertrophic zone that mineralization takes place. When the pyridine nucleotide

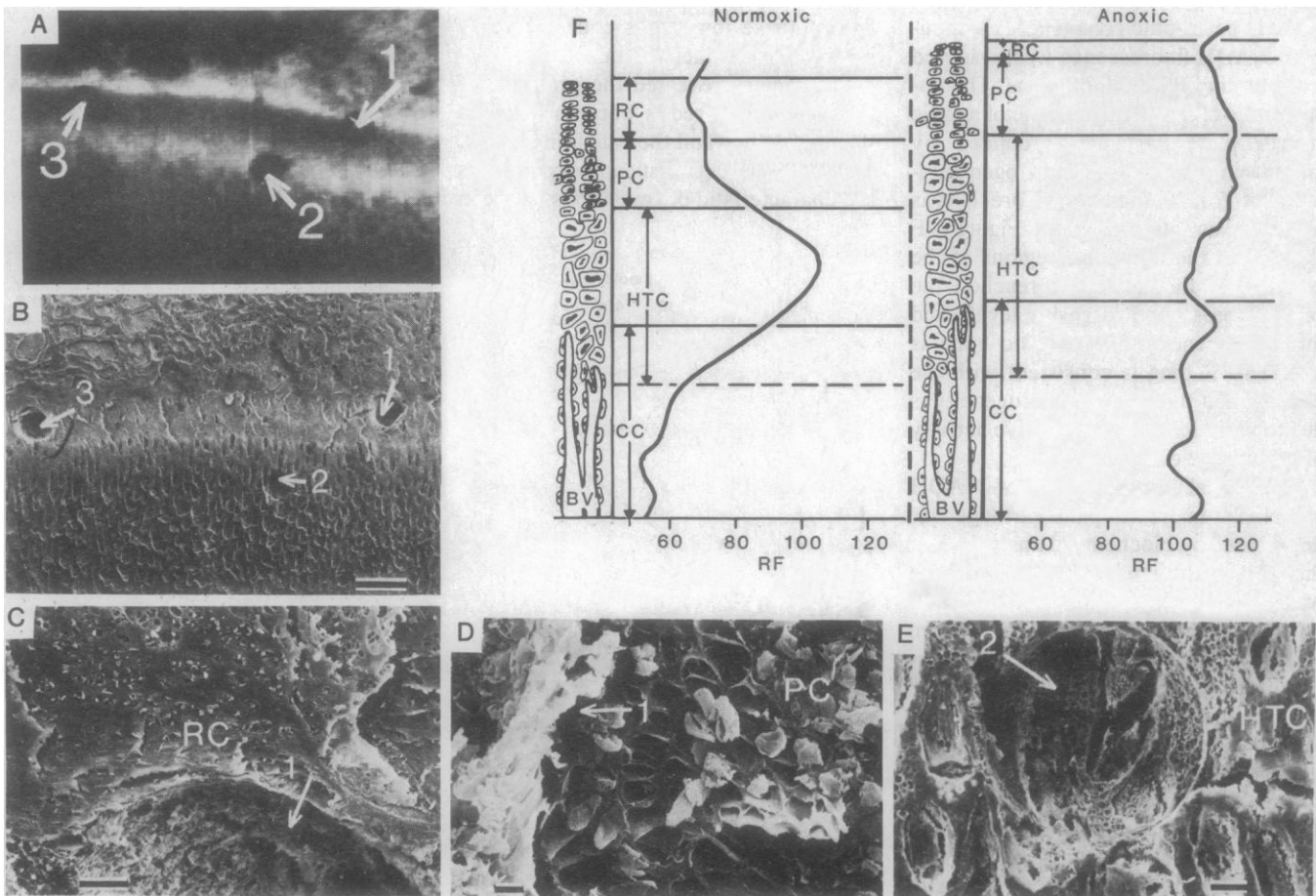


Fig. 1. NADH fluorescence and SEM of growth plate cartilage. (A) Two-dimensional distribution of NADH in the epiphyseal growth plate. The highest level of fluorescence (displayed as a "white" signal), due to the presence of reduced pyridine nucleotides is seen lateral to drill hole 2. Between holes 1 and 2, a low level of NADH fluorescence is seen. The high fluorescence above drill hole 1 does not respond to cellular anoxia and is probably an artifact of tissue preparation. (B) Low-power SEM of chick epiphyseal growth plate showing the cell zones and the three drill holes. Scale bar, 1000 nm. (C) Upper portion of drill hole 1. This region of the hole lies in a zone of resting cartilage (RC). Scale bar, 100 nm. (D) One side of drill hole 1. Lateral to the drill hole is a zone of proliferating cartilage (PC). Scale bar, 10 nm. (E) Drill hole 2. This is shown in relationship to the hypertrophic zone (HTC) and calcifying cartilage (CC). Scale bar, 10 nm. (F) The relative NADH fluorescence (RF) of normoxic and anoxic growth plate cartilage.

scan was matched with tissue morphology, dramatic zone-specific differences in fluorescence were seen (Fig. 1A). Thus, in the hypertrophic cartilage zone, the NADH signal was high. Above this zone and drill hole 2, a low pyridine nucleotide signal was elicited from proliferative cartilage. The lowest NADH signal was obtained from bone and calcified cartilage (below drill hole 2). Between each zone, sharp fluorescent boundaries were observed. A similar fluorescence distribution was seen if the tissue was rapidly frozen in liquid nitrogen or first frozen in Freon-13 or in hexane cooled in liquid nitrogen. A high fluorescence was seen in the tissue zone above drill holes 1 and 3. This zone contained few cells, and the fluorescence of the layer was not influenced by the metabolic state of the tissue. We concluded that this fluorescence band was due to an intrinsic fluorescence of the cartilage matrix and not related to NADH.

When the fluorescence intensity was related to the tissue morphology, the maximum relative fluorescence signal (RF) was recorded in the central region of the hypertrophic zone (Fig. 1F); minimum NADH fluorescence was observed in the resting-proliferating zone. The fluorescence of a separate sample of anoxic growth plate cartilage, produced by maintaining the tissue in a nitrogen environment for 30 minutes before it was frozen, was also studied. Figure 1F shows that the individual regions of the anoxic growth plate have reached the same fluorescence intensity level, and the heterogeneity of normoxic bone is lost. This finding is consistent with the concept that the NADH heterogeneity is due to variations in the oxidative activity of growth plate chondrocytes.

The actual concentration of NADH and  $\text{NAD}^+$  in growth plate cartilage was determined by biochemical analysis. For this part of the study, the frozen tissue was sectioned in a transverse direction on a Jung microtome, and 4 by 30  $\mu\text{m}$  sections were collected, pooled, and lyophilized. The tissue was then analyzed for pyridine nucleotides (7) and for protein (8). Every fifth tissue section (6  $\mu\text{m}$  thick) was stained with hematoxylin-eosin and examined by light microscopy. The pyridine nucleotide concentration in each of the tissue zones of growth plate cartilage is shown in Fig. 2. This figure shows that the ratio of NADH to  $\text{NAD}^+$  is low in the resting-proliferating zone; in the hypertrophic zone, this relation is reversed, and the tissue is very reduced. The relative concentrations of the redox pairs in these two zones corroborate the qualitative and quantitative findings ob-

tained with the fluorimetric scans. The high NADH/ $\text{NAD}^+$  ratio of the hypertrophic zone is comparable to values obtained from glycolytic, hypoxic, and anoxic tissue (9). The similarity of the biochemical measurement of total cell NADH to the fluorescent spatial distribution demonstrates that the mitochondrial redox measurement is a good indicator of the oxidative state of the cell (10).

The functional significance of the NADH concentration in each of the zones of the calcifying growth plate requires discussion. In the hypertrophic zone, the high NADH signal indicates that the mitochondria are in a reduced or resting state; this is probably related to the low tissue  $\text{O}_2$  tension (2). It is in this zone that there is loss of accumulated mitochondrial  $\text{Ca}^{2+}$  and  $\text{P}_i$  and that vesicle mineralization is first detected (1, 2). The finding that there is an increase in the level of reduced pyridine nucleotides in the hypertrophic zone provides direct support for the hypothesis that mitochondrial ion efflux results from a decrease in cellular oxidative activity. Efflux of these ion stores could serve to initiate tissue mineralization.

Fluorimetry revealed the presence of relatively sharp redox borders between the precalcified and the calcifying zones. In nonmineralized tissues, sharp borders are characteristic of transitions between

normoxic and hypoxic tissue volumes. This is particularly evident in model coronary occlusion in freeze-trapped rat hearts where the border zone is 150  $\mu\text{m}$  wide (6). Similarities in border fluorescence of hypoxic soft tissue zones and those observed in our study of calcifying cartilage support the view that hypoxic regions may also exist in the growth plate. While the causes of a localized hypoxia are unknown, possible contributing factors include changes in matrix permeability, high rates of cellular metabolism, and poor vascular supply. Regardless of the cause, localized tissue hypoxia may provide the metabolic signal for the initiation of cartilage mineralization.

IRVING M. SHAPIRO  
ELLIS E. GOLUB  
SABURO KAKUTA

Department of Biochemistry, School of Dental Medicine, University of Pennsylvania, Philadelphia 19104

JOHN HAZELGROVE  
JULIE HAVERY  
BRITTON CHANCE

Department of Biochemistry and Biophysics, Johnson Foundation, University of Pennsylvania

PETER FRASCA  
Orthopaedic Department, Thomas Jefferson University Medical School, Philadelphia 19107

#### References and Notes

1. J. H. Martin and J. L. Matthews, *Clin. Orthop. Relat. Res.* **68**, 273 (1970); H. W. Sampson, J. L. Matthews, J. H. Martin, A. S. Kunin, *Calcif. Tissue Res.* **5**, 305 (1970); C. T. Brighton and R. M. Hunt, *Clin. Orthop. Relat. Res.* **100**, 406 (1974).
2. C. T. Brighton and R. B. Heppenstall, *J. Bone Joint Surg.* **53A**, 719 (1971); A. Boyde and I. M. Shapiro, *Histochemistry* **69**, 85 (1980); C. T. Brighton and R. M. Hunt, *Clin. Orthop.* **100**, 406 (1974).
3. I. M. Shapiro and N. H. Lee, *Metab. Bone Dis. Relat. Res.* **1**, 173 (1978).
4. D. S. Boyd and W. F. Neuman, *Arch. Biochem. Biophys.* **51**, 475 (1954); W. L. Meyer and A. S. Kunin, *ibid.* **129**, 438 (1969); C. Arsenis, *Biochem. Biophys. Res. Commun.* **46**, 1928 (1972); W. L. Meyer and A. S. Kunin, *Arch. Biochem. Biophys.* **156**, 122 (1973); I. M. Shapiro and N. H. Lee, *ibid.* **170**, 627 (1975).
5. B. Chance, B. Schoener, R. Oshino, F. Itshak, Y. Nakase, *J. Biol. Chem.*, in press.
6. B. Quistorff and B. Chance, in *Oxygen and Physiological Function*, F. Jobsis, Ed. (Professional Information Library, Dallas, 1977).
7. T. Kato, S. J. Berger, J. A. Carter, O. H. Lowry, *Anal. Biochem.* **53**, 86 (1973).
8. O. H. Lowry, W. J. Rosebrough, A. L. Farr, R. J. Randall, *J. Biol. Chem.* **193**, 265 (1951).
9. C. Steenbergen, G. Deleuw, J. R. Williamson, *J. Mol. Cell. Cardiol.* **10**, 617 (1978).
10. Recent studies by I. M. Shapiro, M. May, and E. E. Golub, presented at the International Workshop in Calcified Tissues, held in Israel (1982), show that a profound decrease in the energy charge ratio at the site of cartilage calcification. This observation lends support to the view expressed here that there is inhibition of cellular oxidative metabolism at the site of mineralization.
11. Supported by PHS grants DE-02623, 5-R01-AM20020, NS10939, and NS15340. P.F. is the recipient of a career development award (1-KO-4AM-0050402). We thank F. Matschinsky for help with the chemical analysis.

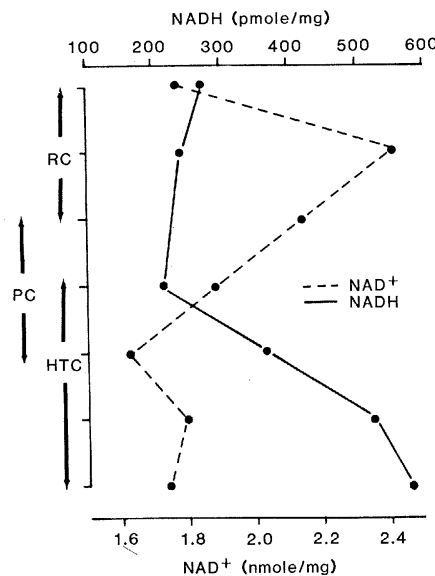


Fig. 2. The pyridine nucleotide content of growth plate cartilage. Cartilage was sectioned on a microtome and pooled tissue slices were analyzed for  $\text{NAD}^+$ , NADH, and protein. The pyridine nucleotide content was related to the morphology of the tissue by staining every fourth section with hematoxylin-eosin and evaluating the section by light microscopy. PC, proliferating cartilage; RC, resting cartilage; HTC, hypertrophic cartilage.